STUDY OF THE SIMPLON AREA GEOTHERMAL ANOMALY IN THE FRAME OF A TRANSALPINE DEEP RAILWAY TUNNEL FEASIBILITY PROJECT

Etude de l'anomalie géothermique de la zone du Simplon dans le but de la réalisation d'un tunnel de base ferroviaire transalpin

B.COPPOLA and F.M.ROSSI, Geological Branch, Ferrovie dello Stato S.p.A., Rome, Italy

R.DI MAIO, D.PATELLA and A.SINISCALCHI, Department of Geophysics and Volcanology, University Federico II, Naples, Italy

L.MARINI and A.MERLA, Geotermica Italiana s.r.l., Pisa, Italy

G.PULELLI, Progeo s.r.l., Forlì, Italy

Abstract: The crossing of huge mountain chains by very deep tunnel excavations, such as in the transalpine railway project across the Simplon area, poses the big question of the high temperatures within the interested rock massif. The local geothermal situations along the Alpine chain are not yet adequately known, but because of the few available data, they are suspected to be very complex. Due to such uncertainties and on account of the great depths implied and the peculiarity of the problem, as a basic approach to understand the actual situation in the Simplon area we have adopted a multidisciplinary procedure, including surface geology lineaments, dipole geoelectric and magnetotelluric deep soundings and physical, chemical and isotope analyses of water samples. In this paper, at first we outline the details of the methods and then disclose the obtained results. The combined interpretation of the whole set of data has allowed to outline a preliminary geothermal model of the explored massif. The study of some geoelectric dispersion effects has finally allowed to predict the range of temperatures referred to the local geothermal anomaly.

Résumé: Le franchissement des grandes chaînes de montagnes en tunnel a forte profondeur, tel que le projet de tunnel transalpin à travers la zone du Simplon, repropose la question des hautes températures au sein des massifs intéressés. La region des Alpes, à ce propos, n'est pas tellement connue et, pour ce qu'on peut dire à l'aide du peu de données disponibles, elle résulte même très complexe. A cause de cette incertitude et du fait des fortes épaisseurs à investiguer, ainsi que des péculiarités des problèmes, afin de comprendre la situation du Simplon on a suivi une approche multidisciplinaire qui réuni, à l'étude géologique classique de surface, des sondages éléctriques dipolaires et magnétotelluriques et une étude géothermale avec analyses physiques, chimiques et isotopiques d'échantillons d'eau des sources existantes en zone. Le travail presenté expose les méthodes d'investigation et les résultats obtenus. L'interprétation combinée de l'ensamble des resultats nous a permis de donner un premier modèle géothermique du massif. L'étude de quelques effects de dispersion géoélectrique nous a finalement permis de prévoir l'interval de température lié à situations d'anomalie thermique locale.

INTRODUCTION

The present paper is a part of the studies that the Italian State Railway Company (Ferrovie dello Stato S.p.A.) has launched in the frame of the feasibility project of a new railway connection between Milan (Italy) and Berne (Switzerland), SSE–NNW trending and about 150 km long across the Alpine chain, in correspondence with the Simplon Pass area. Independently of the final solution for the new railway layout, a tunnel of about 32 km will have to be realized between the river Toce valley (Domodossola, Italy) and the river Rhone valley (Visp–Brig, Switzerland), at elevations ranging from 400 to 700 m a.s.l.

The importance and complexity of this kind of work requires since the beginning the understanding of the general geologic setting about the interested area and of the geologic–technical problems referable to the tunnel excavation, which have to be verified and closely examined in following, more detailed, phases of design.

Thus, a pre–feasibility phase consisting of a bibliographic study, which led to consider a 20 km wide belt from Arona (Italy) to Thun (Switzerland) and whose median axis is traced in fig.0.1, has been carried out. The set of the data collected during this phase allowed the elaboration of a synthetic cross–section along the median axis of the considered belt, here reported in fig.0.2. This section shows a schematic geotectonic reconstruction and the synthesis of the expected main geologic–technical problems across the profile, which were then used to plan the detailed geological studies of the feasibility project, at present still in progress.

The planned schedule of the feasibility project includes all geological topics (tectonics, neotectonics, geomorphology, hydrogeology, seismology and geothermics) as well as a first lot of in situ investigations aimed at a deeper analysis of the raised geologic–technical problems.

According to an optimization criterion of the available financial resources, these investigations were concentrated on a few well–posed problematic aspects, which are particularly relevant in a railway tunnel project, whose problems very often heavily condition the whole railway layout.

Following the above guideline and on the basis of the available preliminary data, two first main categories of problems, deserving further detailed investigations even in the feasibility phase, were individuated:
(a) mechanical properties of the structural setting of the rocks;
(b) hydrogeologic and geothermal conditions.

The first subject has been already dealt with; the main results obtained by the relative field investigations are drawn in a recent paper (Coppola et al., 1993). Thus, this paper is devoted only to the second argument, limited, of course, to the area more closely regarding the new Simplon railway tunnel. To this end, it is worth recalling that the existence of high temperatures inside the Mt.Leone massif (Simplon) was by a long time known since they were observed during the digging of the present operating railway tunnel, which crosses the massif at an average altitude of about 680 m a.s.l. and within which temperatures as high as 55 °C were measured.

According to the deepening level required by the feasibility project, the activities which we are going to present in the following sections,

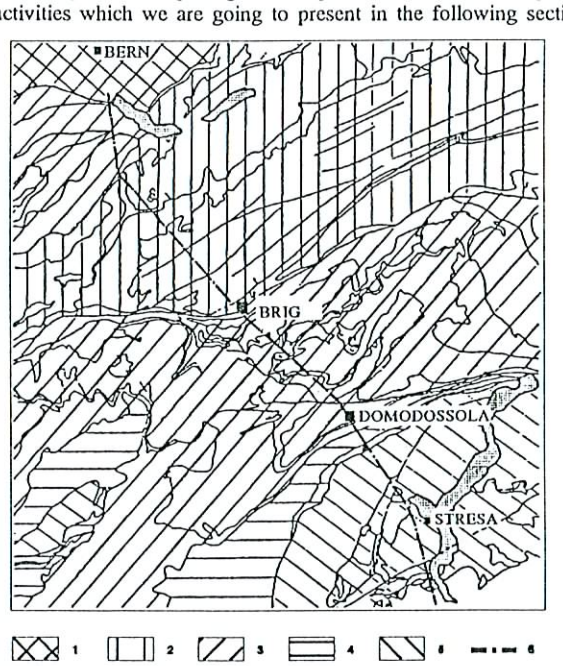

Fig. 0.1 – The main structural units of the Alps in the Simplon area
1: Foreland Units; 2: Helvetic Domain; 3: Penninic Domain; 4: Austro–Alpine Domain; 5: Southern Alps Units; 6: Schematic new railway layout

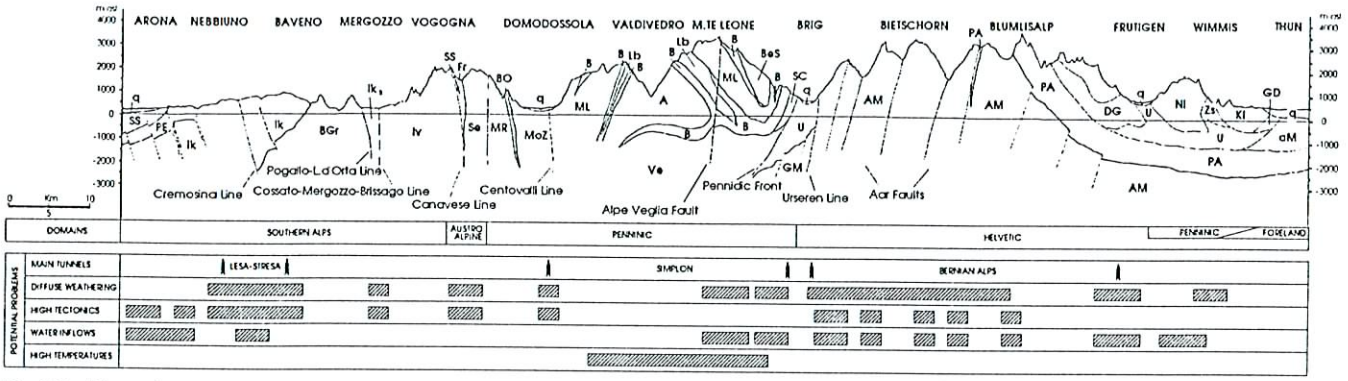

Fig. 0.2 – The main structural units of the Alps along the geotraverse Arona–Thun (redraw after Ente Ferrovie dello Stato, Attività Geologia, 1990) – SS, PE, BGr, IK, IKs, Iv: Southern Alps Units; FR, Sl : Austro–Alpine Units; B, Sc, BO, MoZ, ML, Lb, A, Ve, GD, KI, Zs, NI: Penninic Units; WL, DG, U, PA, GM, AM: Helvetic Units; aM: Foreland Units.

were divided into geophysical and hydrogeologic geochemical field investigations. As it concerns the geophysical contribution, we have carried out dipole geoelectric and magnetotelluric soundings by a combined approach, aiming at ascertaining the possible existence of resistivity dispersion effects referred to local geothermal anomalies. As it regards the hydrogeological–geochemical contribution, we have performed physical–chemical and isotope analyses on water samples collected from cold and thermal springs in the area and then elaborated a model of the water circulation and of the heat exchanges with the rock massif.

1. GENERAL GEOLOGIC OUTLINE

1.1. Genesis and tectonics of the Alpine chain

The genesis of the Alpine chain has been the subject of numerous studies since the end of the last century, but only in the seventies of this century the theoretical research on the evolution of the original Alpine basin (Thetis) has been given a huge impetus, thanks to the introduction of plate tectonics, which has led to a revolutionary interpretation of the Alpine geology.

In this new context, the longitudinal belts, recognizable in the regional development of the Alpine chain by their distinctive morphologic, tectonic and paleogeographic features, can be interpreted as structures ("systems") referable to definite geographic areas ("domains"), which are specified as follows:

- Helvetic Domain (to which the Ultra–Helvetic Domain is associated): it represents a continental belt of the northern european plate, which was involved in a late phase of the Alpine orogeny. The external crystalline massifs, their partially autochthonous covers and a sequence of Mesozoic–Tertiary nappes belong to this domain;
- Pennidic Domain: it defines the outer margin of the European continent, which was originally in contact with the paleoocean of Thetis and heavily involved in the Alpine orogenesis;
- Austro–Alpine Domain: it represents the southern margin of the insubric plate thrust over the Pennidic units during the Alpine orogeny;
- South–Alpine Domain: it consists of the hercynian and pre–hercynian crystalline basement and of the Carboniferous–Tertiary cover of the insubric plate. This domain was marginally interested by the Alpine orogeny, which shows in this area the effects of a brittle tectonics with an almost total lack of metamorphism.

The contacts between the different systems, and between the various units within each system, are of tectonic nature with the presence of cataclastic and/or mylonitic sheets often transformed and rearranged by synorogenetic metamorphic processes mainly in the Pennidic area. It follows that the knowledge of the geostructural relationships between the different units and the nature of their contacts has a decisive importance not only for scientific purposes, but in case of civil works also for predicting and preventing the unavoidable technical problems, which can happen when crossing a rock massif.

The noteworthy geostructural characteristics of the tectonic systems which are encountered along the surface belt under study, are briefly summarized hereafter, proceeding from south to north, according to the direction of the orogenetic thrust.

The Southern Alps outcrop between Arona and Vogogna and comprise rocks of the crystalline basement and of the Tertiary cover mostly not interested by the Alpine metamorphism. The crystalline basement is made up of metamorphic lithotypes pertaining to the units of the Ivrea–Verbano Zone (granulites and kinzigites) and of a series of micaschists and paragneisses interested by hercynian plutons and pre–hercynian gneissic masses (Scisti dei Laghi). These formations are interested by some dislocations of regional character, among which we quote in particular the Cremosina Line, to the north of Arona, which is a pre–Alpine fault, reactivated during the Alpine orogenesis and interesting the Serie dei Laghi, and the Cossato–Mergozzo–Brissago Line,which separates the Serie dei Laghi from the Ivrea–Verbano unit. This last line is dislocated close to Mergozzo by the Pogallo–d'Orta Line, which has the characters of a deep fault in correspondence with which a step in the metamorphic degree between the Serie dei Laghi and the Ivrea – Verbano Zone can be noticed.

The Austrides System outcrops between Vogogna and Cardezza, with upright and partially mylonitized bedding planes (Scisti di Fobello and Rimella); the deformed belt vanishes to the north in the Sesia–Lanzo Zone, which consists of decidedly more compact gneissic lithotypes.

The sequences belonging to the Pennides are met to the north of Cardezza until Brig. From a structural point of view, they are characterized by complex polyphasic foldings, which present, however, an isoclinal character with a differentiated bedding. In the stretch between Cardezza and Domodossola upright outcrops of the upper Pennidic sequences (Monte Rosa Nappe and Moncucco Zone) are present. They essentially consist of orthogneisses and paragneisses associated to amphibolites and secondary lithotypes. To the north of Domodossola the lower Pennidic sequences are met (Antigorio Nappe, Monte Leone Nappe, Lebendun Nappe). These sequences are characterized by a greater structural complexity with tectonic contacts ranging from subvertical to subhorizontal. The contacts which delimit the gneissic masses of the crystalline sequences are generally marked by the presence of marbles, calcschists and micaschists belonging to the Mesozoic cover. Similar Permian–Carboniferous covering lithotypes are met in proximity of Brig, at the northern mouth of the existing railway tunnel. The tectonic lineaments in the Pennides outcropping area seem to have prevailing characters of brittle deformation. The Centovalli Line, which merges to the west into the Simplon Fault, has an E–W trend with subvertical bedding and shows vertical and transcurrent movements. The Simplon Fault, merging south–westward, puts in contact the upper and lower Pennidic units across a cataclased and mylonitised belt. The Alpe Veglia Fault, E–W trending, is of doubtful definition; in fact, although the presence of this tectonic disturbance was observed since the digging of the existing railway tunnel, there are no surface evidences about its lateral continuity westward and its depth extension. Close to Brig, the Pennidic front determines a tectonically very active area, where even recent seismic phenomena have been detected.

The Helvetic units to the north of Brig are made up of paragneisses of the hercynian crystalline basement of the Aar massif and of its Permian–Jurassic cover with variable degree of allochthony.

1.2. Geologic outline of the Simplon area

The Simplon area is characterized by a notable complexity, partially clarified thanks to the field observations made possible by the digging of the existing railway tunnel, performed at the beginning of this century. Fig.1.1 illustrates three SE–NW trending cross–sections, which

synthesize the average structural situation along profiles corresponding with the existing and the hypothesized new railway tunnel layouts.

The reconstruction depicted in fig.1.1 defines a structural scheme characterized by the overlapping of NW-vergent crystalline sequences of the basement separated by intercalations of Mesozoic metacarbonatic rocks. In the area close to Domodossola the structural setting is generally vertical with the Monte Leone sequence superposed over the Antigorio sequence. Proceeding towards north, the structure tends to a subhorizontal bedding with outcrops, for a long distance, of the tectonically lowest sequence (Antigorio Nappe). In the Swiss territory, however, a new straightening of the structure is observed in correspondence with the piling up front of the Pennidic over the Helvetic units. In this zone, the structure consists of north-vergent close foldings. The allowable structural setting is the result of a succession of prevailingly isoclinal deforming phases, partially obliterated by the Alpine metamorphic events. A Late-Alpine deforming history superposed over these events modifying the geometrical relationships between the different units. The structural setting was next complicated by the occurrence of tectonic lineaments of brittle character.

The map of fig.1.2 shows that in the area between Iselle and Gondo there is a system of N-S trending subvertical faults, which develop nearly lengthwise to the hypothesized trend of the new railway layout. The system is made up of fractures with limited vertical throw, which provoke on the surface gravitative slope slidings as well as mass collapses. The potential negative influence of this tectonic system is testified by the technical problems met during the digging of the present railway tunnel at about 4 km after the southern mouth: the rock masses were found heavily weathered and subject to copious water inflows, which reached a global flow rate of about 1000 l/s.

Another problem is represented by the situation of the Alpe Veglia Fault in the central portion of the present railway tunnel close to Mt.Leone. To the presence of this tectonic disturbance are associated the heavy geomechanical problems encountered between 9 and 11 km ahead from the southern entrance to the present tunnel, namely high fracturing of the rock bodies and also strong thrusts to the tunnel walls. Furthermore, in the same zone were observed the highest temperatures both in rock and in water. Even though both lateral continuity and longitudinal extension of the fracture system is still a matter of debate among geologists, the available bibliography and field data seem to support the opinion that the tectonic accident should attenuate proceeding westwards, within the belt under examination.

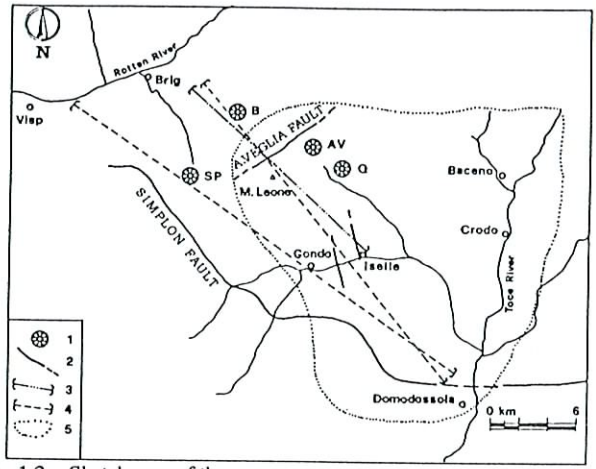

Fig. 1.2 – Sketch map of the survey area
1: DES and MTS stations; 2: Main faults; 3: Present Simplon Tunnel; 4: New Simplon Tunnel layout; 5: Boundary of the hydrogeochemical survey area.

1.3. Internal temperatures

As is well known, the temperature on the earth's free surface represents the energy balance between the terrestrial heat flow and the climatic conditions. Proceeding downwards into the earth, the temperature rises according to a thermal gradient, which is given at any depth as the ratio of the local heat flow over the thermal conductivity of the representative rock.

Generally speaking the space dependence of the above thermal parameters is due to the different lithologic and structural properties of the geological formations. Moreover, the internal temperature distribution can locally diverge from the general model, due to the existence of circulating waters, radioactive minerals, magmatic basins, gas migrations, and so on. More generally, geothermal anomalies can be also due to particular structural conditions of the rock masses under analysis.

As it regards the new tunnel project in the Simplon area, we have at first considered the set of temperatures, observed during the digging of the present Simplon railway tunnel (Biadego, 1906), which are synthetically drawn in fig.1.3. By examining the diagram "a", it appears quite evident that there is a rise of the temperature along the tunnel, in the spacing range from 9 to about 13 km ahead from its southern entrance, and a relative decrease after 4-5 km ahead from the same access. Moreover, along the same horizontal profile the average geothermal gradient ranges between 11.5 and 36 °C/km. The mean geothermal gradient has been calculated, for simplicity, by the relation (T-T')/(h'-h), in which T and h are the measured temperature and the elevation a.s.l. of each sampling point along the tunnel, respectively, and T' and h' are the annual mean temperature and the elevation a.s.l. of each corresponding projected point on the ground surface, respectively. A ready examination of the diagram reveals two anomalies of the geothermal gradient: the first

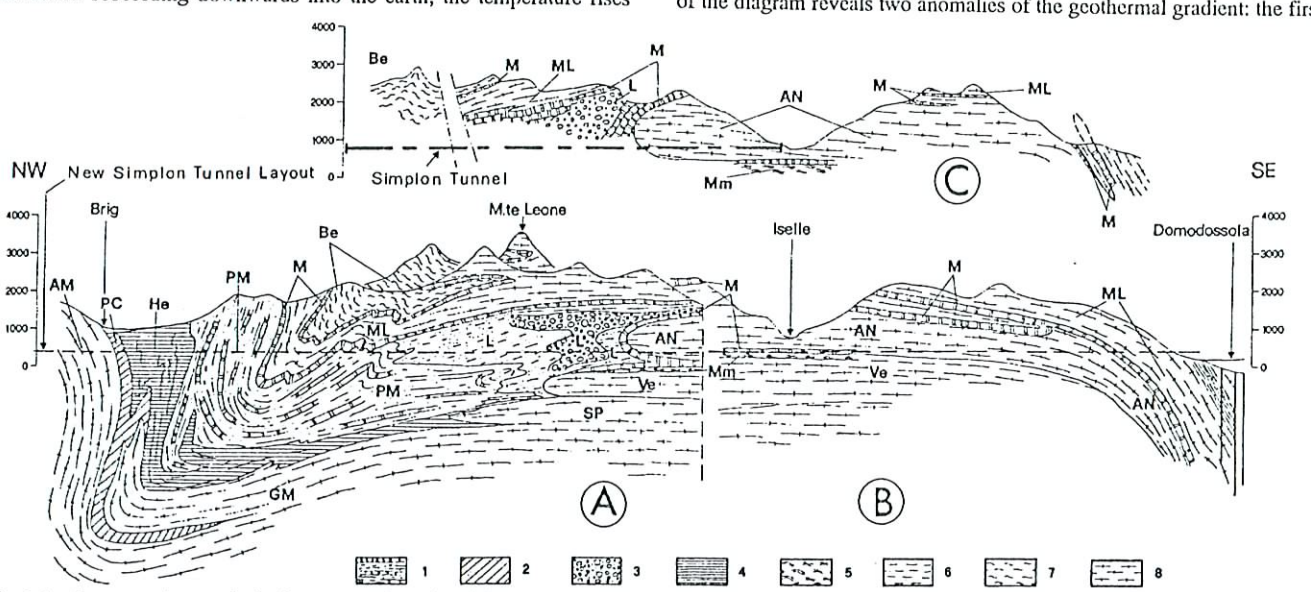

Fig. 1.1 – Interpretative geological cross-sections (modified from Ferrovie dello Stato S.p.A., ISTRA-ITALFERR SIS.T.AV., 1992)
1: Calcschists and marbles with subordinate metapelites; 2: Metaconglomerates and metavolcanites; 3: Conglomeratic and arenaceous gneisses; 4: Predominant marbles with calcschists; 5: Muscovitic micaschists; 6: Carbonatic metapelites; 7: Paragneisses and micaschists; 8: Ortogneisses and metagranitoids AM: Aar Massif AN: Antigorio Nappe Be: Berisal Nappe GM: Gotthard Massif He: Helvetic parautochthonous covers L: Lebendun Nappe M: Mesozoic covers of the penninic nappes ML: Monte Leone Nappe Mm: Mesozoic micaschists of the Baceno-Varzo Zone PC: Permo-carboniferous autochthon of the external massifs PM: North-penninic calcschists SP: Subpenninic units Ve: Verampio granite

negative anomaly corresponds with a narrow band around the distance of 4.5 km from the tunnel southern entrance, and the second positive anomaly in the range from 14 to 15 km from the same entrance.

In the diagram "b" of fig. 1.3 the measured temperatures are compared with the locations and flow rates (point values) of the main inflows intercepted during the digging of the existing railway tunnel. The diagram shows that the greatest falls in internal temperature are observed in correspondence with the most abundant inflows. Conversely, very low water flow rates are related to the highest internal temperatures.

Since such variations cannot be adequately explained by only a correlation with the thickness of the overlying formations, the same must be interpreted as the evidence of some local geothermal anomalies. For this reason the study was finalized to investigate the main features of the geothermal status of the Simplon massif, with particular reference to individuating the geothermal anomalies and to analyzing the thermal exchange properties between rock masses and circulating waters.

2. GEOPHYSICAL STUDY

2.1. Dipole electric soundings

2.1.1 Basic outline of the method

As is well known, the dipolar electric sounding (DES) method consists of the determination of the subsurface resistivity vertical distribution by a set of apparent resistivity values, measured on the ground surface with a couple of separated dipole circuits, of which one is used to inject current into the ground and the other to measure the corresponding voltage. Among the different mutual dispositions of the two dipoles the most used is the axial array, in which the two dipoles are set aligned along a common axis. The axial DES is carried out by progressively increasing the distance between the centres of the two dipoles. One dipole is held fixed, normally the emitting dipole, and the second is shifted along the sounding expansion axis. At every spacing, a determination of the apparent resistivity parameter corresponds. In modelling by a set of buried plane parallel layers (1D interpretation), the vertical line across the midpoint of the fixed dipole is considered as the attribution axis of the layering parameters.

Since at any given exploration depth the two dipoles need a cable length notably shorter than that required by the classical Schlumberger device, all problems related to accessibility in the survey area, cable unwinding, current leakage and em coupling are strongly minimized by the dipolar method. However, DES responses are normally much more perturbed by lateral inhomogeneities than are the Schlumberger responses. Thus, the most suitable approach consists of combining the easiness of the dipolar device in data acquisition and the smoothness of the Schlumberger device in data modelling. This approach requires an intermediate processing step consisting of the transformation of a field dipolar diagram into the equivalent Schlumberger diagram (Patella, 1974; 1984; 1986).

In the Simplon area, we have performed four DES. The centers of the fixed dipole are marked in the map of fig.1.2. The DES are indicated by the initials of the nearest localities, namely DES Q (Quartina), DES AV (Alpe Veglia), DES B (Berisal) and finally DES SP (Simplon Pass).

The attribution centers of the DES coincide with the station sites of the magnetotelluric soundings (MTS), which will be shown in the next section. The requirement of keeping close coincidence between DES and MTS stations arises from one of the main goals of the research: evidencing resistivity frequency dispersion effects across rock volumes, which present alterations due to idrothermal paragenesis. This research topic will be discussed in full detail in the section devoted to the MTS interpretation.

2.1.2 Data acquisition, processing and interpretation

The apparatus necessary to perform dipole electrical soundings is made up of separated current and voltage units. The current unit consists of a dc feeder, sustained by external batteries or motor generator, supplied with automatic polarity inverter, square wave period selector and output current regulator. The output voltages are applied to the current electrodes, consisting of steel stakes grounded at the ends of the cable line of the current dipole. The voltage unit is equipped with a digital multimeter, controlled by a microcomputer, which also serves as a real-time signal stacking processor. The potential drops, created by current circulation in the subsoil, are detected by the receiver unit across two copper-copper sulphate impolarizable electrodes, grounded at the ends of the cable line of the measuring dipole.

In deep electric sounding the voltage message discrimination is often limited by telluric noise contamination. In the cases of low message-to-noise ratios we have applied a message enhancement procedure based on the stacking algorithm, which has the notable advantage of being an in-field ready-to-work method on small computers and of allowing a real-time decision about the message recovering quality, thus avoiding too short or too long recording times (Alfano et al., 1982; Patella, 1985; Lapenna et al., 1987). Trains of square current waveforms of 60 s of period and sampling time of 3 s have been used in the Simplon area. Fig.2.1 shows two examples of stacking diagrams, relative to records with different message-to-noise ratios. For the less corrupted record, an execution time of 1200 s has revealed more than sufficient to indicate a stable asymptotic level, which allows a correct estimate of the noise-free message voltage. On the contrary, in the worse case of the second recording a time duration of about 2300 s has been required to observe a similar stable asymptote.

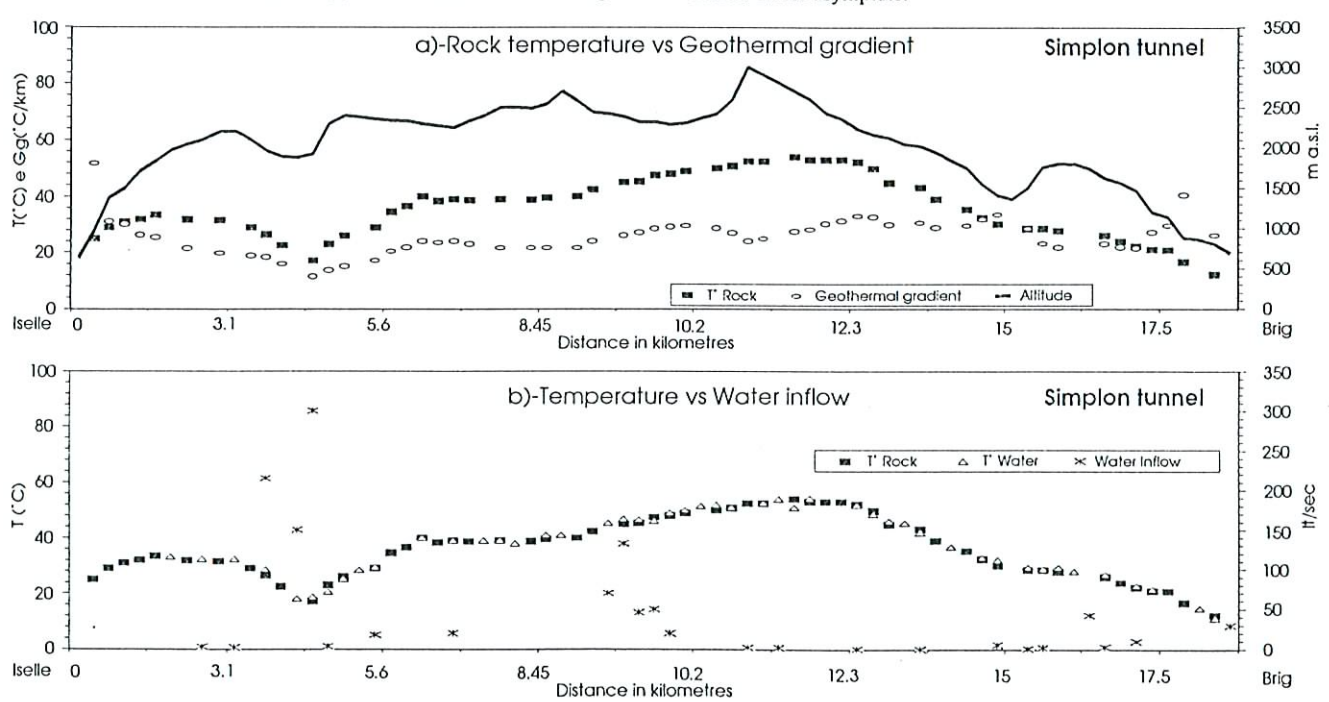

Fig. 1.3 – Temperature vs water inflow during the digging of the present Simplon crossing tunnel

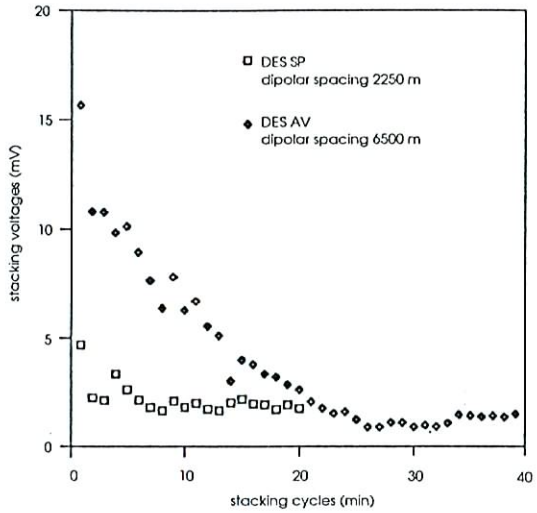

Fig. 2.1 – Two examples of voltage stacking diagrams obtained during the execution of the dipole electric soundings in the Simplon area

The DES apparent resistivities have been then calculated and drawn on log–log diagrams. Fig.2.2 shows the original DES curves (full lines) and the corresponding Schlumberger transform curves (dashed lines). As expected, the DES curves are notably scattered due to lateral disturbances. On the contrary, the transformation has given very smooth Schlumberger curves, readily amenable to 1D modelling. The suggested quantitative interpretations of the DES are indicated in the same fig.2.2.

2.2. Magnetotelluric soundings

2.2.1 Basic outline of the method

In the magnetotelluric sounding (MTS) method, natural electromagnetic fields are used to investigate the electrical conductivity distribution in the subsurface, by analyzing the amplitude, phase and directional cross-relationships between electric and magnetic components of the MT field on the ground surface. By using suitable broadband recording arrays field programs can be designed to investigate regions of interest within the earth, from depths of a few tens of meters down to the upper mantle.

There is a large documentation on the arising of complex polarization phenomena during variable current circulation in rocks and fluids. They are usually referred to as dispersion effects in frequency-domain. The most relevant effect of polarization can be observed in rocks containing mineral and/or clay particles, which fully or partially block fluid filled pores and/or fractures. In many geothermal environments clay and sulphide particles are common alteration products, due to interaction between rock matrices and hydrothermal fluids migrating towards the ground surface.

To diagnose the presence of deep polarization effects, MT is a very suitable method. In fact, as it operates in the frequency-domain and dispersion consists of the variation of resistivity as frequency changes, the existence of a dispersive rock underground will generate anomalous diffusion patterns of the electromagnetic field through it and, accordingly, the MT response is expected to be affected by its presence. There is, however, an important limitation in making MT interpretation, due to the circumstance that any polarization-affected MTS response can be as well interpreted as a polarization-free response. Patella (1987) demonstrated that such an inherent ambiguity can be solved by comparing MTS and DES data collected in the same site. In fact, since the DES technique is unaffected by dispersion as it operates in the steady state or very low frequency current circulation regimes, it can provide an accurate estimate of the zero-frequency resistivity and thickness of the layers. These layering parameters would allow construction of the synthetic dispersion-free MT response for the same layered situation, which is then compared with the actual MTS response. A close matching of synthetic and field MT diagrams would mean that dispersion is not detectable or not existent at all. In the other case, one could admit the presence of dispersion effects, at some definite depths, provided that the discrepancy of the diagrams is consistent with the dispersion phenomenology.

As above mentioned, the dispersion phenomenology in the frequency domain in rocks consists in a resistivity-versus-frequency complex dependence, essentially concentrated in the 0.001–1000 Hz frequency range. The formal behaviour of the dispersion amplitude diagram is a monotonic decrease of resistivity as frequency rises from a zero-frequency asymptote (dc resistivity) to an infinite-frequency asymptote. Among the many models suggested to interpret the frequency dispersion diagrams, the Cole–Cole model (Pelton et al., 1978) is recognized as the most geophysically sound formulation, best fitting to field and laboratory experimental data. The Cole–Cole system is fully described by a set of three parameters: m, τ and c, i.e. chargeability, main time constant and frequency dependence, respectively.

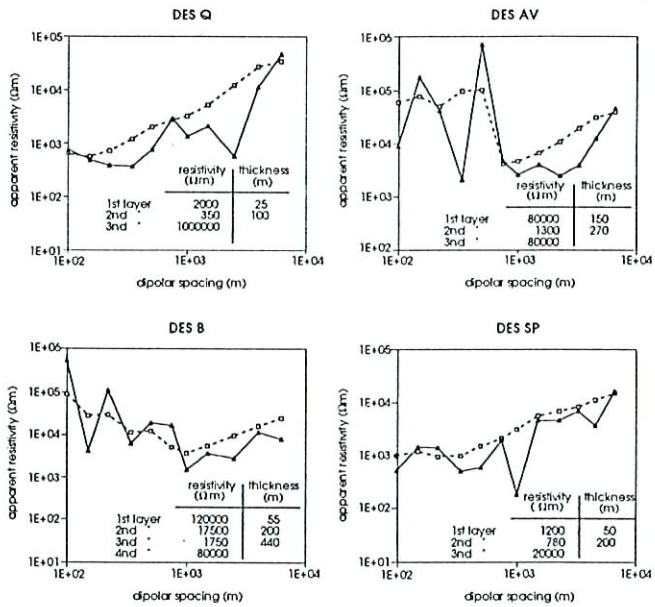

Fig. 2.2 – Dipolar and Schlumberger transformed apparent resistivity diagrams of the four soundings performed in the Simplon area.

2.2.2 Data acquisition, processing and interpretation

The apparatus to carry out MTS measurements consists of induction coil magnetometers, pairs of lead–lead chloride impolarizable electrodes to sense the electric field variations, plus amplifiers, filters and an advanced recording and processing system to permit the signals to be captured and analyzed. In fig.2.3 a block diagram of the MTS field system is sketched.

In the Simplon area we have performed four MTS. The stations coincide with the centers of the DES, as reported in fig.1.2. The MTS are also indicated by the initials of the nearest localities, i.e. MTS Q, MTS AV, MTS B and MTS SP.

The record processing is done in the frequency-domain by the Fast Fourier Transform by which earth impedances to the diffusion waves are computed as functions of frequency and direction. The impedances are next converted into apparent resistivity and phase curves against frequency or period. Two sets of MTS diagrams are obtained according to the orthogonal directions of an opportunely selected reference coordinate x–y system on the ground surface.

Fig.2.4 displays the apparent resistivity and phase diagrams corresponding to the two orthogonal directions for each MTS.

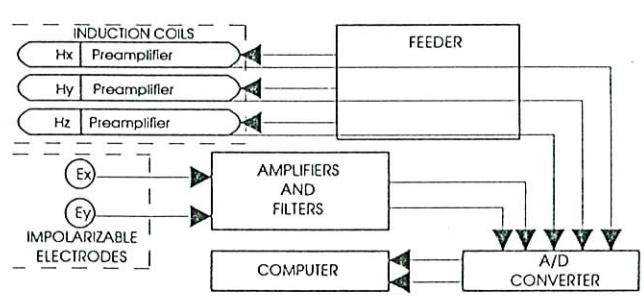

Fig. 2.3 – Block diagram of the magnetotelluric surveying system

The MTS diagrams are then interpreted in terms of electrical resistivity versus depth and sounding position. As previously announced, we have considered the possibility of dispersion effects in the MTS data, disposing of the DES results. A 1D modelling has been attempted and the obtained layering parameters are listed in the same figures depicting the field diagrams. The two orthogonal MTS diagrams are represented by crosses and circles, and the synthetic MT curves, deduced by taking into account the DES results, are represented with solid lines. When a discrepancy has appeared in the left-hand shorter period portion of the curves, evinced by the synthetic curve lying well over the actual MT curve, then the Cole-Cole dispersive parameters have been introduced, in order to obtain a satisfactory matching of the MTS theoretical dispersion-affected curve with the field data set. In fig.2.4 the dispersive layer in the layering parameters sequence is indicated by a star, and the corresponding Cole-Cole parameters are listed immediately below. For more information about the method of construction of a synthetic MTS curve from DES data the interested reader is referred to Patella et al. (1991).

To conclude, we think it worth outlining some considerations about a few distortions appearing in the field diagrams collected in the Simplon area, which can help understand in a more complete way the whole MTS interpretation process. At first we notice that the MTS Q diagram shows a good correspondence between the two orthogonal apparent resistivity curves only in the left-hand branch until the 10 s upper limit. A 1D modelling can only be restricted to this portion, as a 2D structure, at least, would be better indicated to fit the diverging final branches of the curves. As the residing depths of this structure would be completely outside the scopes of this study, we have preferred to limit our attention to a 1D modelling of only the xy MTS apparent resistivity component, which best conforms to the general pattern displayed by all other MTS diagrams obtained in the survey area. Furthermore, we observe a vigorous static shift effect in the MTS SP apparent resistivity diagram. This time, the 1D interpretation is fully justified over the whole period range of analysis, since the static shift is due only to surface resistivity inhomogeneities. The choice of the yx MTS SP apparent resistivity diagram for the 1D modelling has been now suggested by the DES SP interpretation, which has given a set of layer resistivities fully conforming to the yx lower level.

2.3. Temperature indirect estimate

As previously pointed out, the presence of resistivity dispersion effects can be related to geothermal activity. The question roses whether an estimate of the temperature inside the dispersive body can be obtained by a careful analysis of the Cole-Cole dispersion parameters m, τ and c. Although there are experimental evidences suggesting a temperature dependence of the dispersion phenomenon, a close mathematical prediction model is, however, not yet available. In order to arrive at a reliable response to such a special question, we shall tackle the problem from a pure physical point of view and try to take profit by empirical relationships deduced from other controlled temperature field experiments.

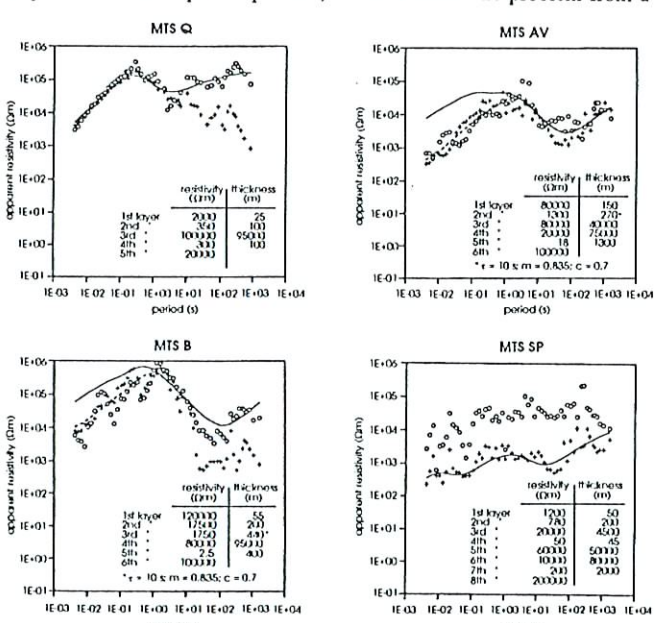

Fig. 2.4 – Magnetotelluric apparent resistivity and phase diagrams of the four soundings performed in the Simplon area

To understand the roles of the Cole-Cole parameters in regulating dispersion effects, we can simplify the problem by considering the analogy which can be established between any elementary cell of the polarizable volume with a parallel resistor-condenser circuit. Also, a simple square wave current excitation is assumed to expose the basic phenomenology. The response to any other current waveform, as e.g. the armonic oscillation typical in MT analysis, can be derived in a straightforward manner from this basic presentation. When a metallic-type mineral particle blocks a pore conduit filled with an electrolytic solution, the electrical current flow through it is no longer regulated by Ohm's law. In particular the occluding element behaves in part as a condenser, and ions of opposite sign accumulate over the fluid-particle upstream and downstream interfaces, and in part as an added resistor along which current circulation is maintained by redox reactions. Thus, the polarization effects correspond to charging or discharging of the condenser-like mineral particles, as soon as the external exciting field is switched on or off, respectively.

The number of disseminated blocking particles along the rock porous system regulates the polarization intensity. The amplitude of the polarization effects increases as the residual ohmic paths of the unblocked capillaries decrease owing to an increase in the number of occluding particles. The chargeability parameter m well expresses the maximum polarization amplitude.

The charging or discharging processes are time dependent relaxation transients. In other words, the response of the polarizable system to the abrupt current excitation or its sharp removal is not instantaneous. In a unimodal ionic solution the transients are analytically described by damping real exponential functions. The time constant τ is a very useful parameter for characterizing the rapidity or slowness of the relaxations.

In a more complex ionic solution where different charge carriers are activated by the electric pulse, the relaxation transient is a more complicated function, which includes the relaxation specific mode of each ionic constituent. The Cole-Cole dispersion model accounts for this multimodal behaviour and introduces a new parameter, the frequency factor c, which gives a close insight of how the constituent unimodal time constants are distributed about the main time constant τ.

Let us go now to consider the role of temperature in modifying the above described Cole-Cole dispersion parameters. It seems likely to admit that with normal variations of temperature inside the system no substantial modification of the total number of polarizable charged carriers should happen. Although the resistance across the ohmic paths in the capillaries is expected to decrease with increasing temperature, due to a decrease of water viscosity and a corresponding increase of ions mobility (Keller and Frischknecht, 1966), no variation of the capacity of the condenser-like blocking metallic grains should arise. Thus, chargeability is expected to be an almost temperature-independent parameter.

Conversely, a rise of temperature produces an enhancement of thermal motion of the metal ions about their equilibrium position in the blocking metallic grain, which interferes with the freedom of movement of the conduction electrons (Keller and Frischknecht, 1966). So a delay in the redox reactions is generated, which corresponds to a rise of the added resistance. The final effect is a direct proportionality of the time constant τ with temperature.

Finally, if we admit, for simplicity, that all ionic constituents of the electrolytic compound have intrinsic time constants depending on temperature through the same proportionality coefficient, also the frequency dependence c should not reveal any substantial variation with temperature.

In conclusion, the Cole-Cole main time constant against temperature relationship is expected to give a relevant information about the thermal status of a buried geologic environment, above which dispersion effects are evidenced e.g. by a combined DES and MTS surveying.

As previously said, an analytical expression of the τ versus T relationship is at present not yet available, and the search of it is outside the purposes of the present paper. Nevertheless, by taking advantage of previous experiments in field situations with known deep temperatures as from boreholes, a reliable solution to our problem can be as well approached. Fig.2.5 depicts the result of our investigation. The τ against T empirical diagram has been drawn by means of data referred to various mining prospectings in USA and Canada (direct estimates of τ by the induced polarization method) (Pelton et al., 1978), and to geothermal prospectings in Oregon and Italy (indirect estimates of τ by the combined DES and MTS analysis) (Patella et al., 1991). If we insert in the diagram

of fig.2.5 the resulting values of τ(10 s) as estimated from the MTS AV and MTS B interpretations, we readily deduce a temperature inside the range 40–85 °C for the recognized dispersive layers.

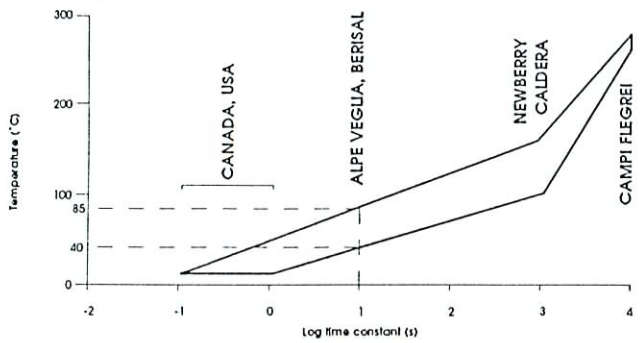

Fig. 2.5 – Temperature–versus–time constant empirical diagram

3. HYDROGEOCHEMICAL STUDY

3.1. Basic outline of the methodology

Based on the experience gained during the excavation of the Simplon tunnel, it has been decided to gather a conspicuous batch of data on temperature distribution, location of water circuits and physical–chemical characteristics of such waters, in order to minimize the risk of unexpected inflows of waters, both cold and hot, possibly CO_2–rich, when the new Simplon tunnel will be digged in the future. Furthermore, knowledge of hydrogeochemical and geothermal features of this area is necessary for deciding waterworks, size of air–pumps, kind of materials that must withstand water corrosion tendency, etc.

The object of this section is to provide an improved version of both the geothermal context and the hydrogeochemical framework of the Simplon area and to derive practical implications for the excavation of the new Simplon tunnel.

3.2. Field work and laboratory analyses

In order to achieve the objectives stated above, a total of 50 water samples were collected from springs of the Ossola district (Fig. 3.1) and analyzed, both chemically and isotopically.

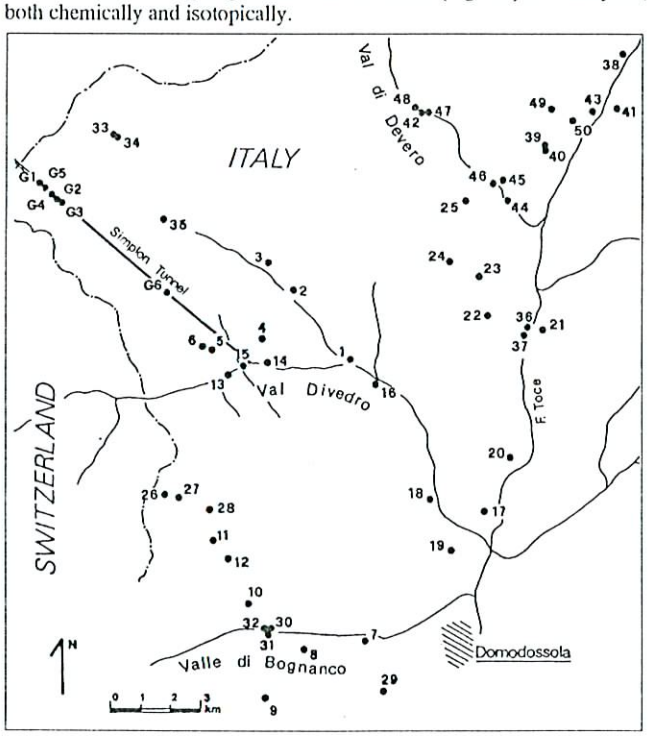

Fig. 3.1 – Location map of the sampled water points

Temperature, pH and alkalinity were measured directly in the field, owing to their unstability.

Other chemical analyses were carried out in headquarters laboratory by means of ionic chromatography (Na, K, Li, Ca, Mg, Cl, NO_3, SO_4), ion–selective electrode (F), colorimetric method (SiO_2) and mass spectrometry (D/H and $^{18}O/^{16}O$ isotope ratios).

Six samples previously taken from different flows inside the Simplon tunnel (Martinotti et al., 1989; Hunziker et al., 1990) have also been considered in data processing.

3.3. Chemical classification of waters

The square plots of Langelier and Ludwig (1942), (e.g. Fig. 3.2) and the triangular cross–sections of the corresponding compositional pyramids (e.g. Fig. 3.3) have been used for the chemical classification of sampled waters. The square plots of Langelier and Ludwig constitute the bases of these pyramids and display the relative contents (eq %) of the seven main ionic species (Na, K, Ca, Mg, HCO_3, SO_4, Cl), leaving ionic salinity out of consideration. The triangular cross–sections allow one to consider the relationship between composition and ionic salinity. This approach is particularly useful for our purposes as it allows one to identify families of waters whose characteristics can be easily related to leaching of lithotypes present in the area.

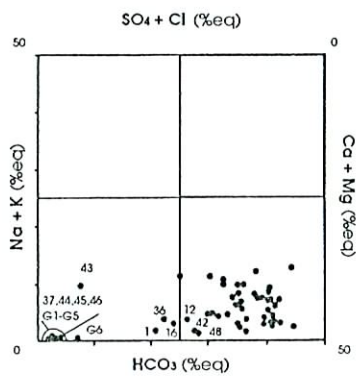

Fig. 3.2 – Langelier–Ludwig square plot

The characteristics of the hydrogeochemical types identified in the area are listed hereunder.

The calcium bicarbonate type of low ionic salinity comprehends most of the sampled cold springs, which are generally characterized by outlet temperature in the 4 to 12 °C range and ionic salinity in the 0.4 to 3 meq/l interval. These waters are related to shallow and relatively quick circuits mainly located into gneissic rocks.

Only two samples can be ascribed to the magnesium bicarbonate type of low ionic salinity. They are San Bernardo di Bognanco (sample 11) and Alpe Lusentino (sample 29). Their temperature and ionic salinity are within the ranges typical of the previous hydrogeochemical type. Also these waters come from shallow and relatively fast circuits; however the prevalence of magnesium over calcium suggests that these waters experience leaching of ophiolites (serpentinites, metagabbros, prasinites, amphibolites), which actually crop out near these two springs.

The soda–water spring of Alpe Veglia (sample 33, temperature 7.2 °C, ionic salinity 26 meq/l) can be referred to the calcium bicarbonate type of high ionic salinity, whereas the two soda–water springs of Bo–

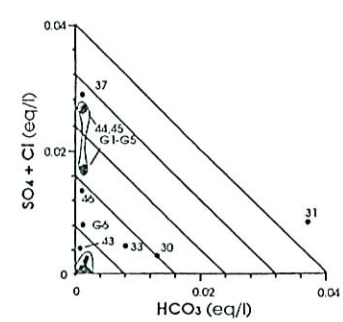

Fig. 3.3 – E–W cross–section of the Langelier–Ludwig composition pyramid whose base is the square plot of Fig. 3.2

gnanco, named San Lorenzo (sample 31, temperature 12.3 °C, ionic salinity 92 meq/l) and Ausonia (sample 30, temperature 10.5 °C, ionic salinity 32 meq/l) belong to the magnesium bicarbonate type of high ionic salinity. Compositional differences between the soda–water of Alpe Veglia and those of Bognanco are due to interaction with different lithotypes: the gneiss are responsible of the calcic character of the first, whereas the ophiolites are the cause of the magnesian character of the second ones.

All these waters exhibit partial pressures of carbon dioxide (P_{CO2}) close to 1 bar. These very high P_{CO2} values are likely due to uprising of CO_2–rich gases of deep origin along important tectonic structures, such as the Simplon–Centovalli fault, at Bognanco, and the Alpe Veglia fault in the homonymous site. The high P_{CO2} makes these waters very aggressive for the rocks they contact, and it is responsible for their high bicarbonate– and cation–contents.

The calcium sulfate type of high ionic salinity includes the thermal waters of the Simplon tunnel (samples G1 to G5, temperature between 20.7 and 40.8 °C, ionic salinity in the 37 to 56 meq/l range), the Valle d'Oro spring of Crodo Spa (sample 37, temperature 11.8 °C, ionic salinity 60 meq/l) and the springs of Baceno–Uresso (samples 44, 45 and 46, temperature in the 9.7 to 12.4 °C interval, ionic salinity between 30 and 55 meq/l).

The chemical features of these waters are due to dissolution of the anhydrite and/or gypsum contained into the carbonate metasedimentary rocks of Mesozoic age. These lithotypes actually crop out nearby the springs of this hydrogeochemical type and are associated with the inflows of thermal waters in the Simplon tunnel (e.g. Jacquier, 1905).

These are meteoric waters that percolate through a body of rocks of about 1600 m in vertical thickness, taking heat from the rocks and approaching the condition of thermal equilibrium with them. This interpretation is supported by both:

- the temperature profile measured during the excavation of the tunnel (Fig. 1.3a/b), which shows a relative minimum where the thermal waters are found, suggesting that their effect was "to cool the tunnel rather than to heat it" (Clark and Niblett, 1956);
- the low P_{CO2} values of these thermal waters (0.0014 to 0.0032 bar), which is similar to that of the cold water inflow in the Simplon tunnel (0.0015 bar).

The calcium sulfate bicarbonate type of intermediate ionic salinity comprehends sample G6 of the Simplon tunnel, representative of a large cold water inflow (temperature 7.2 °C, ionic salinity 19 meq/l), and the following springs: Lisiel of Crodo Spa (sample 36), Fontana di Varzo (sample 1), Molino di Varzo (sample 16), Valle Devero 1 (sample 42) and Valle Devero 2 (sample 47), which exhibit temperature between 8.1 and 9.7 °C and ionic salinity in the 4.4 to 9.7 meq/l range.

The chemical and physical features of these waters are intermediate between those of the calcium sulfate type of high ionic salinity and those of the calcium bicarbonate type of low ionic salinity. Their origin can be therefore explained by one of the two following hypotheses:

- quick circulation into carbonate metasedimentary rocks of Mesozoic age; the rapidity of the circulation does not allow an effective heat transfer from rock to water and hinder the dissolution of gypsum and anhydrite;
- mixing between calcium sulfate waters of high ionic salinity and calcium bicarbonate waters of low ionic salinity.

The hypothermal spring of Piedilago (sample 43, temperature 16.1 °C, ionic salinity 10 meq/l) can be referred to the calcium sodium sulfate type of intermediate ionic salinity. The chemical characteristics of this water are intermediate between those of the calcium sulfate type and those of the sodium (calcium) sulfate type. Waters ascribable to the latter type are not represented in the area under examination, but discharge at (Vuataz, 1982):

- Bagni di Craveggia, 20 km ENE of Domodossola, outlet temperature 27 to 28 °C, and
- Brigerbad, 4 km WSW of Brig, outlet temperature 37 to 53 °C.

Both thermal sites are fed by relatively deep aquifers, whose maximum temperature is estimated to be 85 °C and 110 °C, respectively (Martinotti et al., 1989).

3.4. Stable isotopes of water

Inspection of the classic deuterium vs oxygen–18 correlation plot (Fig. 3.4) shows that sampled waters define the following regression line:

$$\delta D = 8.22\ \delta^{18}O + 13.58 \qquad (3.1)$$

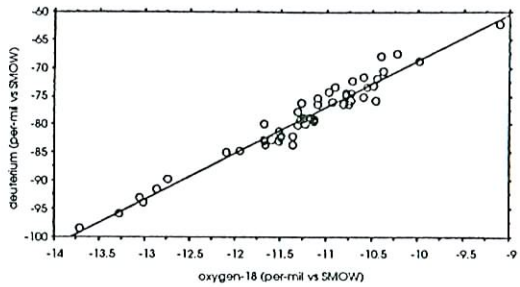

Fig. 3.4 – Deuterium vs oxygen–18 correlation plot

which is not very different from the worldwide meteoric water line, (Craig, 1961).

The lack of significant enrichments in both oxygen–18 and deuterium excludes the occurrence of both rock–water exchange at high temperature and surface evaporation.

The variations in isotope values is thus mainly caused by differences in the elevation of the zones of meteoric infiltration. In spite of the remarkable scatter observed in the correlation plot of oxygen–18 vs elevation of discharge (Fig. 3.5), the two following constraints can be considered in order to derive a simple relationships between isotope values and average altitude (h_i) of the zones of meteoric infiltration:

- the chemical characteristics of the water inflows sampled in the Simplon tunnel indicate that these waters infiltrate where the carbonate metasedimentary rocks of Mesozoic age crop out above the tunnel and then percolate through these lithotypes towards the tunnel; the average elevation of these outcrops is about 2300 m a.s.l., both for the thermal waters (samples G1 to G5) and for the cold water (sample G6); it must be underscored that the homogeneity in the altitude of infiltration reflects in the homogeneity in isotope values;
- the second constraint is defined by the characteristics of the springs located at highest elevation in the area; their altitude of infiltration is unknown, but can not be much different from the altitude of discharge, as suggested by geographical evidence.

Based upon these two constraints, the following equation can be obtained:

$$h_i = -245.47\ \delta^{18}O - 840.09 \qquad (3.2)$$

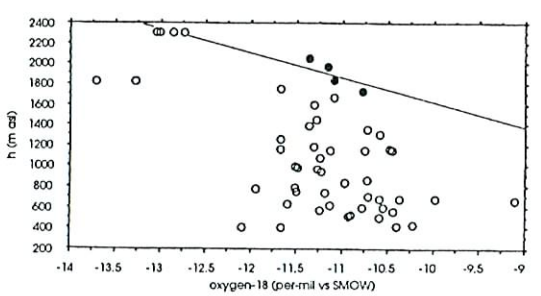

Fig. 3.5 – Correlation plot of oxygen–18 vs elevation

3.5. Geothermal considerations

3.5.1 The thermal anomaly of the Ossola district

The existence of a thermal anomaly in the Ossola district is supported by:

- the presence of the thermal springs of Piedilago, Bagni di Craveggia and Brigerbad;
- the high temperatures measured in the Simplon tunnel, which appear anomalous if compared with those found in the nearby Gottardo and Loetschberg tunnels.

This thermal anomaly is likely caused by the quick uplift which affected in Plio–Quaternary times the crustal block sited north of the Simplon–Centovalli tectonic line, with respect to the block located south of it (Martinotti et al., 1989).

3.5.2 Rock–water heat transfer in the Simplon tunnel

The regular trend in the temperature–distance profile (Fig. 1.3/b), measured during the excavation of the Simplon tunnel, is strongly upset by two main water inflows, which are located:

- at 9.5–10.5 km from the northern portal (water temperature 30 to 49 °C, flow rate 300 l/s);
- at 4.5 km from the southern portal (water temperature 10 to 14 °C, flow rate 1000 l/s).

These temperature and flow rate values were measured when the tunnel was dug. The different temperature of these two main water inflows likely reflect a different permeability and a diverse kind of circulation, although both inflows are fed by waters which percolate through carbonate metasedimentary rocks. On the one hand, the waters of the thermal inflow move quite slowly and remain close to the water–rock thermal equilibrium condition; this is likely due to a relatively low permeability and a relatively high surface of heat transfer between rock and water. On the other hand, the waters of the cold inflow move quite quickly, perhaps along fractures enlarged by karst; the rock–water heat transfer is thus less efficient than in the previous case. It can not be ruled out, however, that the cold water inflow is the product of mixing between waters that percolate through carbonate metasedimentary rocks and waters that interact with fractured gneissic rocks.

3.5.3 Geothermal evidence provided by sampled springs

Further information on the thermal regime in the subsoil of the surveyed region is provided by sampled springs. Inspection of the temperature vs elevation plot (Fig. 3.6) shows that most sampled springs distribute along the regression line, and well above the local line of air temperature changes with elevation. Springs 15 (Iselle 2, T = 14.2 °C) and 43 (Piedilago, T = 16.1 °C) are, instead, well above the regression line and must be considered thermally anomalous. Also spring 17 (Crevola d'Ossola, T = 16.0 °C) seems to be thermally anomalous, but it is probably affected by anthropic effects and should be left out of consideration. Apart from these three springs, the strict correlation between temperature and elevation suggests that all these springs are fed by shallow circuits. However, the fact that their temperature is significantly higher than local air temperature deserves further analysis. Therefore, the altitude of infiltration (h_i) has been evaluated for each spring, on the basis of isotope data, by means of equation (3.2). The average annual temperature of infiltrating water (T_i) has been estimated assuming thermal equilibrium with atmospheric air. The "effective" geothermal gradient, egg, has then been calculated through the following relationship:

$$egg = (T_S - T_i) / (h_i - h_S) \qquad (3.3)$$

where T_S and h_S refer to the temperature (in °C) and altitude (in m) of each spring. The "effective" geothermal gradient exhibits bimodal frequency distribution (Fig. 3.7). In spite of the complex meaning of this parameter, the family characterized by mode of about 11 °C/km can be considered representative of thermal anomalies, probably caused by conductive heat transfer from relatively hot rocks or waters located under the shallow water circuits. Restricting our consideration to the cluster of anomalous springs only, it must be underscored that these clusters are sited in the following zones, that are therefore thermally anomalous:

- Iselle – Bugliaga (4 samples)
- Alpe Veglia – Nembro (3 samples)
- Piedilago – Spotigene (3 samples).

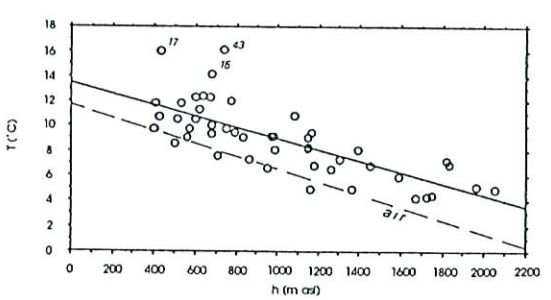

Fig. 3.6 – Correlation plot of temperature vs elevation

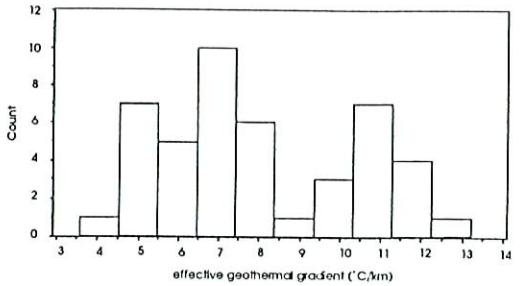

Fig. 3.7 – Frequency distribution of the "effective" geothermal gradient

3.6. Practical implications

Available thermometric and hydrogeochemical data allow one to draw the following practical implications relevant for the excavation of the new Simplon tunnel:

(1) The temperature value at a given depth, in dry rocks, can be evaluated assuming an average geothermal gradient of 28°C/km. Therefore the maximum expected temperature at about 2300 m below the surface (elevation 2700 m a.s.l.; average annual air temperature –2.1 °C) is close to 63°C.

(2) Temperature values lower than in dry rocks are expected in zones of water inflow; the higher is the water flow rate, the lower is the temperature expected.

(3) Zones of water inflow are foreseen in carbonate metasedimentary rocks and in fractured rocks.

(4) The dissolved salt content of these waters depends upon temperature, partial pressures of carbon dioxide (P_{CO2}) and the lithotypes in which the waters circulate. However, maximum expected salinity is 2 g/l or so, based on the chemical characteristics of the waters sampled both at the surface and in the Simplon tunnel.

(5) Acid waters rich in CO_2 (similar to those of Bognanco and Alpe Veglia) can be found where the tunnel will cross important tectonic structures. These waters can have a certain corrosion and scaling tendency.

(6) The water richest in CO_2 (Ausonia spring, Bognanco; CO_2 = 0.096 mol/l) would have a P_{CO2} close to 6.6 bar under the maximum temperature value expected at depth . One liter of this hypothetical water would exsolve 1.8 l of CO_2 upon depressurization at 1 bar with temperature of 0°C. Although this is an obviously hypothetical case, the risk of CO_2 exsolution from CO_2–rich waters must be seriously considered.

CONCLUSIONS

The studies and field investigations so far performed, about the subject of the internal temperatures of the Mt.Leone massif, have brought to light some useful evaluation elements, which are herebelow summarized.

- Temperature values observed in the present Simplon railway tunnel in the range between 30 and 55 °C for the most part of the tunnel length;
- Estimated mean geothermal gradient values, referred to the tunnel height (650–685 m a.s.l.), ranging from 11.5 to 36 °C/km;
- Presence of apparent geothermal gradient anomalies, in the same railway tunnel, about 4.5 km ahead (negative anomaly due to water percolation) and in the space range from 14 to 15 km ahead from the southern mouth;
- Presence of resistivity dispersion phenomena in the MTS AV station site (inside the interpreted depth range 255–695 m, corresponding to the altitude range 905–1245 m a.s.l.) and in the MTS B station site (inside the interpreted depth range 150–420 m, corresponding to the altitude range 1200–1550 m a.s.l.);
- Absence of resistivity dispersion phenomena in the MTS SP and MTS Q station sites;
- Important water percolations within the massif with circulation inside carbonatic bodies;
- Expected salinity value at the altitude of the new railway tunnel of the order of 2 g/l.

These elements have brought us to point out some conclusive remarks, which we are still evaluating in view of the planning of new more refined investigations:

(a) in absence of anomalies, extrapolating the data measured in the present operating tunnel by the calculated mean geothermal gradient, the internal temperatures along the new Simplon railway tunnel should be around 63°C;

(b) the resistivity dispersion phenomena affecting the MTS B and MTS AV diagrams could very likely be related to the presence of the Alpe Veglia fault, which passes between the two MT station sites (see fig.1.2) and was crossed by the present operating Simplon railway tunnel;

(c) the temperature-versus-time constant correlation of the dispersion anomaly about the MTS B site, which is closest to both the operating railway layout and the eastern solution of the project layouts, would indicate a temperature not less than 40 °C at elevations a little higher than that of the present tunnel, where a little lower temperature (38 °C) was measured. We deduce that, in this place, the temperature will vary versus depth according to a very low gradient: therefore, the temperature in the new tunnel should have values a little higher than 40 °C;

(d) the MTS SP station site, located over the western extension of the Alpe Veglia fault (see fig.1.2) has not evidenced any resistivity dispersion phenomenon. We could infer that this fault does not continue westwards. Such a possibility has been already hypothesized by some researchers in the field of Alpine geology;

(e) the overall characteristics of the sampled waters indicate a model of a practically descending circulation, generally in thermal equilibrium with the rock masses, but locally with some cooling action;

(f) with reference to the salinity of the percolating waters and particularly to the carbon dioxide content, we observe that the residing of this gas in acqueous solutions depends on temperature and pressure. Such occurrence must be taken in due account as to the actual possibility of release of gaseous carbon dioxide from strongly carbonatic waters during the digging, especially in conditions of high temperatures. As an example, if the carbon dioxide richest waters, with measured concentration of 0.096 mol/l, would be intercepted during the new tunnel digging at the expected temperature, to which correspond partial pressures of carbon dioxide of about 6.6 bar, we would expect exsolution of carbon dioxide at the rate of 1.8 l per 1 liter of water, upon normal conditions. This aspect has to be carefully analyzed in the near future, due to the serious concerns it can breed.

In conclusion, the results so far obtained, even if they are not exhaustive as it regards the study of the temperature distribution inside the Mt.Leone massif, have nevertheless given useful evaluation elements, mainly concerning the water circulation and thermal exchange model. Accordingly, the research has also put in clear evidence the existence of some thermal anomalies in the Alpe Veglia zone, deduced from the integrated interpretation of the geolectric and magnetotelluric soundings B and AV. In the case in which the correlation of such anomalies with the Alpe Veglia discontinuity should be confirmed by future investigations, the lack of electrical dispersion anomaly in the station site SP would indicate the lack of westward continuity of the Alpe Veglia fault, which therefore should not intersect the westernmost railway tunnel layout of the Simplon project. Last but not least, the potentially risky situation due to the presence of carbon dioxide rich circulating waters in a high temperature environment, deserves a depeer analysis about the hydrogeologic and geothermal regime inside the concerned massif.

References

Alfano, L., Carrara, E., Pascale, G., Rapolla, A. and Roberti, N., (1982), Analysis procedure and equipment for deep geoelectrical soundings in noisy areas. *Geothermics*, 11, 269-280.

Biadego G.B. (1906), *I grandi trafori alpini : Frejus, S.Gottardo, Sempione ed altre gallerie*. Hoepli p.1228

Clark S.P. Jr and Niblett E.R. (1956), Terrestrial heat flow in the Swiss Alps. Monthly Notices of the Royal Astronomical Society. *Geophysical Supplement*, 7, 176-195.

Coppola, B., Di Maio, R., Furani, M., Patella, D., Pulelli, G. and Rossi, F.M., (1993), Indagini geofisiche per la caratterizzazione preliminare dei terreni interessati da progetti di gallerie ferroviarie. Un caso pratico. *Proceedings of the 18th Meeting of Geotechnics, AGI*, Rimini.

Craig H. (1961). Isotopic variations in meteoric waters. *Science*, 133, p. 1702-1703

Ente Ferrovie dello Stato, Attività Geologia, (1990), *Valico del Sempione: studio di prefattibilità (unpublished report)*.

Ferrovie dello Stato S.p.A., ISTRA-ITALFERR.SIS.T.AV., (1992), *Studio geologico-tecnico relativo allo studio di fattibilità Sempione-Gottardo (unpublished report)*.

Hunziker J.C., Martinotti G., Marini L. and Principe C. (1990), The waters of the Simplon tunnel (Swiss-Italian Alps) and of the adjacent Ossola district (Italy): geothermal considerations. *Geothermal Resources Council Transactions*, 14, 1477-1482.

Jacquier M. (1905), *Rapport sur les travaux du tunnel du Simplon*. Ed. Bernard.

Keller, G.V. and Frischknecht, F.C., (1966), *Electrical Methods in Geophysical Prospecting*. Pergamon Press, Oxford.

Langelier W.F. and Ludwig H.F. (1942), Graphical methods for indicating the mineral character of natural waters. *JAWWA*, 34, 335.

Lapenna, V.A., Satriano, C. and Patella, D., 1987, On the methods of evaluation of apparent resistivity under conditions of low message-to-noise ratio. *Geothermics*, 16, 487-504.

Martinotti G., Merla A., Hunziker J.C., Marini L., Guidi M. and Valleggi G. (1989), Valutazione delle potenzialità geotermiche della zona dell'Ossola (Alpi Ocidentali). Contract n. 87.02393.59, *C.N.R.-P.F.E. report*, 42 p.

Patella, D., (1974), On the transformation of dipole to Schlumberger sounding curves, *Geophysical Prospecting*, 22, 315-329.

Patella, D., (1984), Smoothing noise-degraded electrical soundings in shallow and deep investigation studies, *IEEE Transactions on Geoscience and Remote Sensing*, GE-22, 712-715.

Patella, D., (1985), Recenti sviluppi nelle metodologie di acquisizione ed interpretazione di dati geoelettrici dipolari profondi in aree geotermiche, *Proceedings of the Ist Seminar of Actualization*, IILA, Rome

Patella, D., (1986), Low-pass filtering of noisy field Schlumberger sounding curves. Part I: Theory, *Geophysical Prospecting*, 34, 109-123.

Patella, D., (1987), Tutorial: Interpretation of magnetotelluric measurements over an electrically dispersive one-dimensional earth, *Geophysical Prospecting*, 35, 1-11.

Patella, D., Tramacere, A., Di Maio, R. and Siniscalchi, A., (1991), Experimental evidence of resistivity frequency dispersion in magnetotellurics in the Newberry (Oregon), Snake River Plain (Idaho) and Campi Flegrei (Italy) volcano-geothermal areas, *Journal of Volcanology and Geothermal Research*, 48, 61-76.

Pelton, W.H., Ward, S.H., Hallof, P.G., Sill, W.R. and Nelson, P. H., (1978), Mineral discrimination and removal of inductive coupling with multifrequency IP, *Geophysics*, 43, 588-609.

Vuataz F.D. (1982), Hydrogéologie, géochimie et géothermie des eaux thermales de Suisse et des Régions Alpines limitrophes. Matériaux pour la Géologie de la Suisse - *Hydrologie* n. 29, 174 p.